Journal of
Applied Remote Sensing

RemoteSensing.SPIEDigitalLibrary.org

Endmember initialization method for hyperspectral data unmixing

Rui Wang
Hengchao Li
Wenzhi Liao
Xin Huang

SPIE.

Rui Wang, Hengchao Li, Wenzhi Liao, Xin Huang, "Endmember initialization method for hyperspectral data unmixing," *J. Appl. Remote Sens.* **10**(4), 042009 (2016), doi: 10.1117/1.JRS.10.042009.

Endmember initialization method for hyperspectral data unmixing

Rui Wang,[a,b] Hengchao Li,[a,*] Wenzhi Liao,[b] and Xin Huang[c]
[a]Southwest Jiaotong University, School of Information Science and Technology, West Hi-Tech Zone, Chengdu 611756, China
[b]Ghent University, Department of Telecommunications and Information Processing, (TELIN), Sint-Pietersnieuwstraat 41, Ghent 9000, Belgium
[c]Wuhan University, State Key Laboratory of Information Engineering in Surveying, Mapping, and Remote Sensing, No. 129 Luoyu Road, Wuhan 430079, China

Abstract. Spectral unmixing aims at finding the spectrally pure constituent materials (also called endmembers) and their respective fractional abundances in each pixel of the hyperspectral image scene. One important issue in hyperspectral data unmixing is the initialization of endmembers. Most unmixing methods initialize their endmembers by randomly selecting a specified number of pixels from the data or by vertex component analysis, which limits their performance in practice. We propose an endmember initialization method for hyperspectral data unmixing. Our initial endmembers include some of the true endmembers, which improves the accuracy of hyperpspectral unmixing effectively. The experimental results on both synthetic and real hyperspectral data illustrate the superiority of the proposed method compared with other state-of-the-art approaches. [DOI: 10.1117/1.JRS.10.042009]

Keywords: hyperspectral data; unmixing; nonnegative matrix factorization; nuclear norm; initialization.

Paper 16116SS received Feb. 10, 2016; accepted for publication Jul. 22, 2016; published online Aug. 9, 2016.

1 Introduction

Owing to the limitation of spatial resolution together with microscopic material mixing and multiple scattering, an observed pixel in a scene of hyperspectral imagery (HSI) may contain distinct materials, resulting in the so-called mixed pixels. To some extent, the existence of mixed pixels will restrict the exploitation, processing, and applications of HSI in practice. To alleviate this problem, hyperspectral unmixing is often incorporated into the data processing chain. Technically, spectral unmixing aims at decomposing the measured spectrum of each mixed pixel into a collection of constituent spectral (endmembers) and a set of corresponding fractions (abundances).[1]

Conventional unmixing techniques based on a linear mixing model (LMM) can be classified into two categories: the geometrical and statistical approaches.[2] Classical geometrical kinds of approaches further include pure pixel-based and minimum volume-based algorithms. Specifically, the pure pixel-based algorithms, such as the well-known N-finder algorithm (N-FINDR)[3] and vertex component analysis (VCA),[4] assume that there is at least one pure pixel per endmember in the observed data. However, this requisite may not hold in many real scenarios. The minimum volume-based algorithms (e.g., minimum volume simplex analysis[5] and minimum volume enclosing simplex[6]) tend to seek a mixing matrix **W** that minimizes the volume of the simplex defined by its columns. These geometrical methods start with endmember extraction and then perform abundance estimation by decomposing the mixed pixels with the nonconstrained or constrained least square methods.[7] Nevertheless, the abundance estimation is highly dependent on the accuracy of endmember extraction.

*Address all correspondence to: Hengchao Li, E-mail: lihengchao_78@163.com

1931-3195/2016/$25.00 © 2016 SPIE

The statistical kinds of approaches exploit the statistical properties of the data to simultaneously obtain the endmembers and their corresponding abundances. Two typical examples are independent component analysis (ICA)[8,9] and nonnegative matrix factorization (NMF).[10] Specifically, ICA treats hyperspectral unmixing as a blind source separation problem and supposes the spectral components to be mutually independent. But this assumption goes against the abundance sum-to-one constraint (ASC), which degrades the performance of ICA in unmixing. Alternatively, NMF decomposes hyperspectral data into two nonnegative matrices, respectively, corresponding to the endmember matrix and the abundance matrix. The underlying nonnegative constraint automatically ensures the nonnegativity of the estimated abundance fractions. However, due to the nonconvexity of the objective function, NMF may find local minima as the final result. To address this issue, various extensions have been proposed by imposing certain constraints on NMF. These include the use of the smoothness constraint on both endmembers and abundances,[10] the minimum volume constraint,[11] and the piecewise smoothness and sparseness constraints.[12]

For most statistical-based unmixing approaches, proper initialization of endmembers can help to avoid being trapped in local minima. Reference 13 investigated the impact of initialization on endmember extraction, showing that endmember extraction algorithms are sensitive to initial endmembers and that a properly selected set of initial endmembers can improve the searching process significantly. As we know, random initialization and VCA initialization are among the most popular choices for endmember initialization.[14] The latter provides a more accurate initial point by utilizing VCA to identify the endmembers from the real-observed HSI. In addition, N-FINDR results have been used as endmember initialization to decompose mixed pixels in Ref. 15, which has proven to be effective. However, the accuracy of the extracted endmembers by VCA and N-FINDR will be affected by many situations (e.g., the absence of pure pixels/spectra or the HSI with a high mixture).

An improved version of NMF unmixing (NMFupk)[16] employs known materials to formulate the prior knowledge of spectral signatures. The spectral signatures of the known materials, which are associated with the true endmembers, can be obtained from the spectral library and are learned in advance by experiences. The more empirical evidence that is given, the more effective unmixing results can be. However, in many real applications, very limited prior information is available, which limits the performance of this method.

Sparse hyperspectral unmixing aims at finding an optimal set of endmembers in the spectral library that can best model the mixed pixels in the scene.[17] However, the noise in hyperspectral data and the high mutual coherence of a spectral library may deteriorate its performance. In practical applications, the endmembers estimated by sparse unmixing methods are more than the true endmembers or are not true endmembers. Identifying true endmembers in the estimated endmembers is very necessary and useful.

In this paper, we propose an initialization method for hyperspectral data unmixing [named vertex component analysis and norm change (VCANC)]. Our proposed VCANC method initializes the endmembers from both real HSI and the spectral library. First, VCA[14] is utilized to extract the endmembers from the observed HSI. Simultaneously, we propose a method called norm change (NC) to locate the endmembers from the spectral library by exploiting the change of nuclear norm of the estimated sparse abundance matrix. Then we compare the spectra of endmembers obtained by NC with those extracted from the observed HSI by VCA. Finally, to obtain the initial endmembers for postspectral unmixing, we replace some extracted endmembers obtained by VCA with the estimated ones by NC that are similar to each other. The main contributions of the paper can be summarized as follows.

- We propose to evaluate the norm change of an abundance matrix for identifying the endmembers from the spectral library. The initial abundance matrix obtained by a sparse unmixing method is very sparse (i.e., many of its rows are zero vectors). The main idea of locating endmembers from a spectral library is because the nuclear norm of an abundance matrix is changed a lot when a row associated with the true endmember is deleted, whereas it does not change noticeably after deleting any of the other rows.
- In addition, the initial endmembers obtained by the proposed VCANC include not only true endmembers (from the spectral library), but are also related to the real hyperspectral

scene (by VCA), which overcomes both limitations of sparse unmixing and unsupervised VCA.[14] This way, our proposed initialization method enables better performances for the hyperspectral data unmixing.

Numerical experiments on both synthetic and real data demonstrate the efficiency of the proposed VCANC algorithm. This paper is organized as follows. In Sec. 2, we briefly review LMM and NMF. In Sec. 3, we detail our proposed methods on both endmembers identification from the spectral library (i.e., NC) and the final endmember initialization method (i.e., VCANC). In Sec. 4, experimental results on simulated and real hyperspectral data are given. Finally, the conclusions of the paper are drawn in Sec. 5.

2 Background

In this section, we will briefly introduce two basic concepts: LMM and NMF. The former lays a solid foundation for linear spectral unmixing techniques, while the latter is utilized as an example of statistical-based unmixing approaches to testify to the proposed endmember initialization algorithm.

2.1 *Linear Mixing Model*

The proposed method is based on the LMM, where each pixel is described as a linear combination of endmembers with their associated abundances. Formally, the LMM was given by

$$\mathbf{x} = \mathbf{W}\mathbf{h} + \mathbf{n}, \tag{1}$$

where $\mathbf{x} \in \mathbb{R}^{L\times 1}$ is an observation vector at a single pixel with L spectral bands. $\mathbf{W} = [\mathbf{w}_1, \mathbf{w}_2, \cdots, \mathbf{w}_r] \in \mathbb{R}^{L\times r}$ is the endmember reflectance matrix, having $\mathbf{w}_j$ to represent the spectral signature of the j-th endmember. $\mathbf{h} = [h_1, h_2, \cdots, h_r] \in \mathbb{R}^{r\times 1}$ denotes the abundance vector, which corresponds to the proportions of the endmembers in the mixed pixel, moreover, $\mathbf{n} \in \mathbb{R}^{L\times 1}$ is the noise vector. The abundance vector should satisfy ASC and the abundance nonnegativity constraint. Considering the whole hyperspectral data, the LMM can be presented in matrix form as follows:

$$\mathbf{X} = \mathbf{W}\mathbf{H} + \mathbf{N}, \tag{2}$$

where $\mathbf{X} \in \mathbb{R}^{L\times N}$, $\mathbf{W} \in \mathbb{R}^{L\times r}$, $\mathbf{H} \in \mathbb{R}^{r\times N}$, and $\mathbf{N} \in \mathbb{R}^{L\times N}$ are the hyperspectral data, endmember, abundance, and noise matrices, respectively.

2.2 *Nonnegative Matrix Factorization*

Up until now, NMF has been widely used for hyperspectral data unmixing.[10–12,14–16] It aims at decomposing the hyperspectral data into a nonnegative endmember and abundance matrices by minimizing a cost function, i.e.,

$$\min_{\mathbf{W},\mathbf{H}} \|\mathbf{X} - \mathbf{W}\mathbf{H}\|_F^2, \quad \text{subject to } \mathbf{W}, \mathbf{H} \geq 0, \tag{3}$$

where the operator $\|\cdot\|_F$ denotes the Frobenius norm. The iterative algorithm for NMF applied to the problem in Eq. (3) alternates between the following two steps:

$$\mathbf{W} \leftarrow \mathbf{W}. * \mathbf{X}\mathbf{H}^T./\mathbf{W}\mathbf{H}\mathbf{H}^T \tag{4}$$

and

$$\mathbf{H} \leftarrow \mathbf{H}. * \mathbf{W}^T\mathbf{X}./\mathbf{W}^T\mathbf{W}\mathbf{H}, \tag{5}$$

where $(\cdot)^T$ denotes the matrix transpose, and $.*$ and $./$ represent the element-wise multiplication and element-wise division, respectively. With the nonnegative initialization, the updates of

Eqs. (4) and (5) can keep the nonnegativity of $\mathbf{W}$ and $\mathbf{H}$. Moreover, this algorithm has provable convergence.[18]

3 Proposed Endmember Initialization Method for Hyperspectral Data Unmixing

For most statistical-based unmixing methods (including NMF[10] and its extensions[11,12,14]), proper initialization can help to avoid being trapped in local minima. In Ref. 14, the impact of different endmember initializations has been experimentally analyzed, showing that VCA initialization will contribute to a better estimate of abundances than will random initialization, besides achieving a relatively smaller standard deviation. However, when the pixel purity assumption does not hold in the observed scene, VCA fails to extract good approximations of true endmembers from real HSI. As is known, it is certain to find one part or the whole set of true endmembers through the sparse unmixing methods from the spectral library even though they suffer from some limitations.[17] Therefore, these true endmembers can be utilized in the endmember initialization. Here, we propose an endmember initialization method which combines the extracted endmembers by VCA with the true endmembers identified from the spectral library to provide a more accurate initial point.

Since a mixed pixel in a hyperspectral scene is typically represented by very few endmembers of the spectral library, the fractional abundance matrix is very sparse. Ideally, nonzero rows in the abundance matrix correspond to the true endmembers. Nevertheless, due to inevitable limitations of sparse unmixing, the number of spectra with nonzero abundance is much more than that of true endmembers. Mathematically, to delete some linearly dependent row does not noticeably change the rank of the abundance matrix. As such, we choose the nuclear norm as a surrogate for the matrix rank[19] and propose to utilize the nuclear norm change to identify the true endmembers from the library by deleting the rows of the abundance matrix one by one.

Suppose $\mathbf{S}_0 \in \mathbb{R}^{p\times N}$ denotes the abundance matrix estimated by the sparse unmixing method such as the CLSUnSAL,[20] and $\mathbf{S}_i \in \mathbb{R}^{(p-1)\times N}$, $i = 1,2,\ldots,p$ and is the abundance matrix obtained by deleting the i-th row from $\mathbf{S}_0$. For any matrix $\mathbf{S} \in \mathbb{R}^{p\times N}$, its nuclear norm is calculated as follows:

$$\|\mathbf{S}\|_* = \sum_{i=1}^{\min(p,N)} \sigma_i, \tag{6}$$

where $\sigma_i[0 \le i \le \min(p,N)]$ are singular values of abundance matrix $\mathbf{S}$ and then we define δ_i as the norm difference, i.e.,

$$\delta_i = \|\mathbf{S}_0\|_* - \|\mathbf{S}_i\|_*. \tag{7}$$

When the i-th row of $\mathbf{S}_0$ belongs to the true endmember, δ_i will be a relatively large value. The larger the δ_i, the higher the possibility that $\mathbf{S}_i$ corresponds to the true endmember. So the differences $\{\delta_1, \delta_2, \cdots, \delta_p\}$ can be sorted in descending order for ranking the possibility of different signatures. Therefore, we propose an endmember extraction method based on the change of norm (NC), Fig. 1 shows the flowchart of our proposed NC method. Actually, there is more than one signature corresponding to the same material in a spectral library. To ensure that every estimated endmember in $\mathbf{W}_{\mathrm{NC}}$ is related to one material, we only reserve the endmember with the largest δ per material. When there are r endmembers in $\mathbf{W}_{\mathrm{NC}}$, the NC procedure ends.

Since the sparse unmixing methods suffer from the usually high mutual coherence of the spectral library, and from the noise effect, the proposed NC will identify some false endmembers as not being related to the real hyperspectral scene, i.e., not true endmembers. On the contrary, VCA extracts endmembers from the observed HSI, although they are just approximations to pure endmembers. To overcome these limitations, our proposed initialization method (VCANC) combines the endmembers extracted by VCA from the real HSI and that located by NC from the spectral library. Suppose we have r distinct materials in the hyperspectral scene (i.e.,

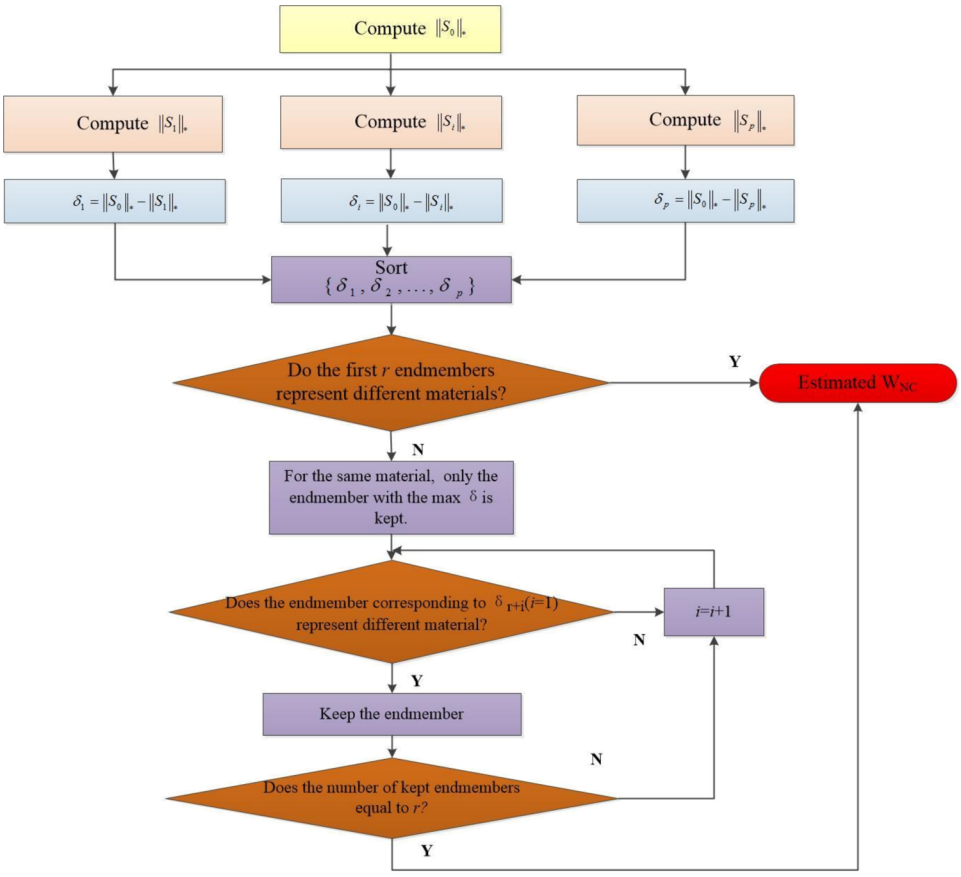

Fig. 1 The flow chart of the proposed NC.

r endmembers), let $\mathbf{W}_{\mathrm{VCA}} = \{\mathbf{w}_{\mathrm{VCA}}(i), i = 1,2\ldots, r\}$ denote the r endmembers from the real hyperspectral data using VCA, and $\mathbf{W}_{\mathrm{NC}} = \{\mathbf{w}_{\mathrm{NC}}(j), j = 1,2\ldots, r\}$ represent the endmembers estimated from the spectral library. Denoted by $\theta(i, j)$, the similarity between the i-th endmember extracted using VCA and the j-th endmember estimated via NC

$$\theta(i,j) = \frac{\mathbf{w}_{\mathrm{VCA}}(i)^T \mathbf{w}_{\mathrm{NC}}(j)}{\|\mathbf{w}_{\mathrm{VCA}}(i)\|_2 \|\mathbf{w}_{\mathrm{NC}}(j)\|_2}, \qquad i,j \in [1,\ldots,r]. \tag{8}$$

The larger $\theta(i, j)$, the more similar $\mathbf{w}_{\mathrm{VCA}}(i)$ and $\mathbf{w}_{\mathrm{NC}}(j)$. This means that the approximated endmember from the real HSI is very similar to the pure endmember from the spectral library. As such, the former can be replaced by the latter to ensure that some true endmembers (i.e., pure spectra) are included in the initialization. Conversely, smaller $\theta(i, j)$ indicates the higher possibility that $\mathbf{w}_{\mathrm{NC}}(j)$ may not be related to the real hyperspectral scene, which is then not included for initialization. After the similarity matrix θ is obtained, the matching procedure of $\mathbf{W}_{\mathrm{VCA}}$ and $\mathbf{W}_{\mathrm{NC}}$ mainly consists of the following four steps.

- Step 1: For every row of θ, we keep the largest value and set others to zeros for the purpose of selecting a signature having the largest similarity with each VCA endmember from $\mathbf{W}_{\mathrm{NC}}$.
- Step 2: To avoid matching multiple VCA endmembers with the same NC endmember, this step retains the largest value for every column of θ and set others to be zeros such that the matched pair with the largest similarity for every NC endmember is obtained.
- Step 3: To guarantee the similarity between the signatures of each matched pair, the thresholding operator is further performed to θ, i.e.,

Algorithm 1 The proposed VCANC endmember initialization method.

Input:

The number of the endmembers r, the spectral library $\mathbf{A} \in \mathbb{R}^{L\times p}$;

The observed HSI $\mathbf{X} \in \mathbb{R}^{L\times N}$;

Output:

The initialization of endmember signature matrix $\mathbf{W} = \{\mathbf{w}(i), i = 1,2\ldots, r\}$;

1: Estimate $\mathbf{W}_{\mathrm{NC}} = \{\mathbf{w}_{\mathrm{NC}}(i), i = 1,2\ldots, r\}$ by NC from the spectral library $\mathbf{A}$ according to the procedure in Fig. 1;

2: Extract endmembers $\mathbf{W}_{\mathrm{VCA}} = \{\mathbf{w}_{\mathrm{VCA}}(i), i = 1,2\ldots, r\}$ from the observed HSI $\mathbf{X} \in \mathbb{R}^{L\times N}$ by VCA;[4]

3: for $i = 1:r$

Compute $\theta(i,j)$, $j = 1,2,\ldots, r$ according to Eq. (7)

4: end for

5: Obtain $\mathbf{W}$ by the matching method introduced from Steps 1 to 4.

$$\theta(i,j) = \begin{cases} \theta(i,j), & \text{if } \theta(i,j) > \text{th}, \\ 0, & \text{if } \theta(i,j) < \text{th}, \end{cases} \tag{9}$$

where th is the given threshold. As a result, the matched pair is kept if the similarity is bigger than this threshold, otherwise, it is abandoned.

- Step 4: Finally, nonzero entries of θ are located for every matched pair. For example, if $\theta(i,j)$ is not equal to zero, the i-th endmember in $\mathbf{W}_{\mathrm{VCA}}$ is matched with the j-th endmember in $\mathbf{W}_{\mathrm{NC}}$. Then we replace the matched endmember in $\mathbf{W}_{\mathrm{VCA}}$ using

$$\mathbf{w}_{\mathrm{VCA}}(i) = \mathbf{w}_{\mathrm{NC}}(j). \tag{10}$$

The algorithmic procedure of the proposed initialization method is formally stated in Algorithm 1.

The obtained endmembers by Algorithm 1 are very much related to the real hyperspectral scene and contain pure spectra, which can overcome both limitations of the VCA and current sparse unmixing methods. In the proposed method, the computational cost has mainly come from the sparse unmixing and norm computation. These two parts will increase the computational cost, but improve the performance of unmixing especially for the data in which there is no pure pixel. When applying our initialization method to most statistical-based unmixing approaches where the initialization is necessary, they can produce a better unmixing performance.

4 Experimental Results

In this section, a series of experiments on both synthetic and real hyperspectral data are conducted. The proposed method is compared to the following methods: (1) NMF with random initialization (Random), (2) NMF with N-FINDR[3] initialization (N-FINDR), and (3) NMF with VCA initialization[4] (VCA). In our VCANC method, CLSUnSAL[20] is used to obtain the initial abundance matrix. The initialization and stopping criterion for the CLSUnSAL are given according to Ref. 20, for which the number of maximum iterations and the tolerance error are set to 200 and $1e$-6. The experimental results are quantitatively evaluated by spectral angle distance (SAD) and root-mean-square error (RMSE).[14,21] Specifically, the SAD is used to measure the similarity of the k-th endmember signature $\mathbf{W}_k$ and its estimate $\hat{\mathbf{W}}_k$, given by

$$\mathrm{SAD}_k = \arccos\left(\frac{\mathbf{W}_k^T \hat{\mathbf{W}}_k}{\|\mathbf{W}_k\|\|\hat{\mathbf{W}}_k\|}\right). \tag{11}$$

The RMSE quantifies the accuracy of the abundance estimation, which is calculated as follows:

$$\mathrm{RMSE}_k = \left(\frac{1}{N}|\mathbf{H}_k - \hat{\mathbf{H}}_k|^2\right)^{\frac{1}{2}}, \tag{12}$$

where $\mathbf{H}_k$ and $\hat{\mathbf{H}}_k$ are the true abundance and the estimated abundance for the k-th endmember signature. Generally speaking, the smaller SAD and the RMSE are, the more accurate the estimation is. In our experiment, the maximum iteration number and the tolerance error of the NMF-based unmixing method are set to 500 and $1e$-4, respectively.

4.1 *Experiments on Synthetic Data*

4.1.1 *Synthetic data creation*

For quantitative comparison, experiments are first conducted on the simulated hyperspectral images. To this end, we generate the same $m \times m$ abundance map as that in Ref. 11: (1) r spectral signatures (laboratory-measured absolute reflectances) are randomly selected from the widely used the U.S. Geological Survey (USGS) digital spectral library as the endmembers. These endmembers are associated the abundance map to synthesize an $m \times m \times L$ (spatial $\times$ spatial $\times$ spectral) HS image; (2) for a given purity (e.g., 0.9), we discard the pixels with abundance fractions larger than the purity and replace them with a mixture composed by all endmembers with abundances of $1/r$; (3) The simulated HS image is degraded by zero-mean Gaussian noise, with a certain SNR (signal-to-noise).

Specifically, we generate three simulated hyperspectral data sets in Table 1 to analyze the robustness of different initialization methods on different noise levels (simulated data 1, named SD1). and different number of endmembers (simulated data 2, named SD2). To compare with NMFupk,[16] simulated data 3 (SD3) is generated for which purity is set to 1.

4.1.2 *Experiment 1 (the choice of threshold)*

Threshold th, which is used to match $\mathbf{W}_{\mathrm{VCA}}$ with $\mathbf{W}_{\mathrm{NC}}$, is very important for the VCANC initialization. In this experiment, the selection of the threshold is based on the similarity between $\mathbf{W}_{\mathrm{NC}}$ and $\mathbf{W}_{\mathrm{VCA}}$. The matching method is tested using different values of th: 0.900, 0.950, 0.980, 0.990, and 0.995. Table 2 shows the number of matched endmembers achieved by the matching method with SD1 when SNR = 15 dB. From Table 2, we can see that the numbers of matched endmembers are very stable when the threshold changes from 0.900 to 0.990 and one endmember is lost when th is set to 0.995. In this table, we only report the results under the condition of SNR = 15 dB; a similar situation may occur with different noise levels when th is set to 0.995. Therefore, we set the threshold to 0.990 in our experiments to guarantee the similarity between $\mathbf{W}_{\mathrm{NC}}$ and $\mathbf{W}_{\mathrm{VCA}}$ and to match the true endmembers as much as possible.

Table 1 Simulated hyperspectral images.

	Parameters			
Simulated data	r	Purity	SNR	m
SD1	5	0.8	From 15 to 45 dB, step 5 dB	64
SD2	From 3 to 8, step 1	0.8	25 dB	64
SD3	5	1	25 dB	64

Note: r, the number of endmembers; m, the spatial size of hyperspectral image.

Table 2 The number of matched endmembers with different thresholds ($n_{W_{NC}}$ denote the number of W_{NC}).

	Threshold				
$n_{\mathbf{W}_{NC}}$	0.900	0.950	0.980	0.990	0.995
4	3	3	3	3	2

4.1.3 *Experiment 2 (robustness analysis to noise)*

In this experiment, the NMF-based unmixing algorithm with four different initializations is performed on SD1. Figure 2 demonstrates that all methods fail when more noise is added to the simulated HS images (i.e., lower SNR) and the results are worst when using random initialization. RMSE values of the proposed VCANC method are slightly better than that of VCA and N-FINDR at high noise levels, but the SAD values are obviously superior to that of the other methods.

4.1.4 *Experiment 3 (generalization to the number of endmembers)*

This experiment evaluates the performances of the NMF-based unmixing method using four different initializations with SD2. The experimental results are shown in Fig. 3. Overall, the performances of all the initialization methods decay when the number of endmembers increases. When adopting random initialization, the SAD and RMSE are worst compared with other initializations. However, the VCANC method produces the best results among all the unmixing results as the number of endmembers increases. Especially for the SAD, VCANC is still obviously better than the other initializations.

From the results of experiments 2 and 3, we can conclude the following findings: (1) It is better to avoid using random initialization for hyperspectral unmixing because the performance is worst in each case; (2) VCA and N-FINDR fail to obtain accurate results when there are no pure pixels in SD1 and SD2; (3) the endmembers estimated by VCANC are related to the observed data and part of them are true endmembers, so VCANC can give more accurate initial points than other initialization methods. In other words, VCANC can relax the requirement of pure pixels in the VCA method and the influence of high mutual coherence of the spectral library on sparse unmixing; and (4) VCANC initialization can contribute to a better estimation of endmembers.

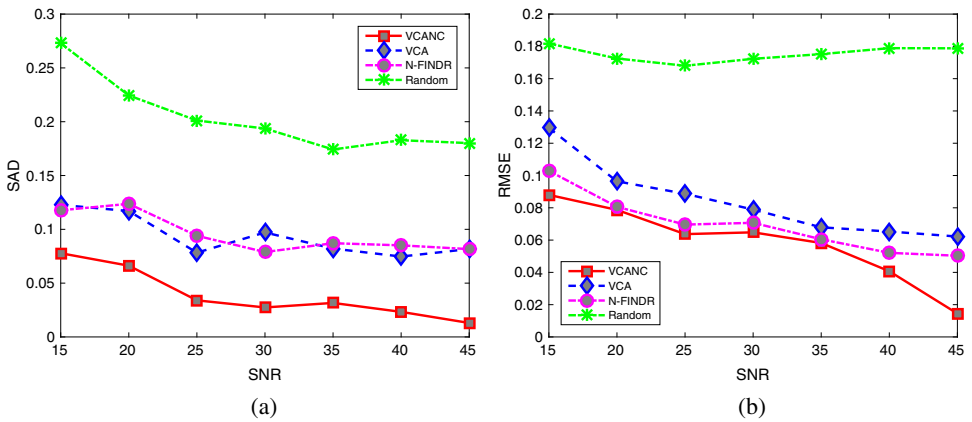

(a) (b)

Fig. 2 Comparison of the algorithms with different noise levels of hyperspectral data (SD1). (a) SAD and (b) RMSE.

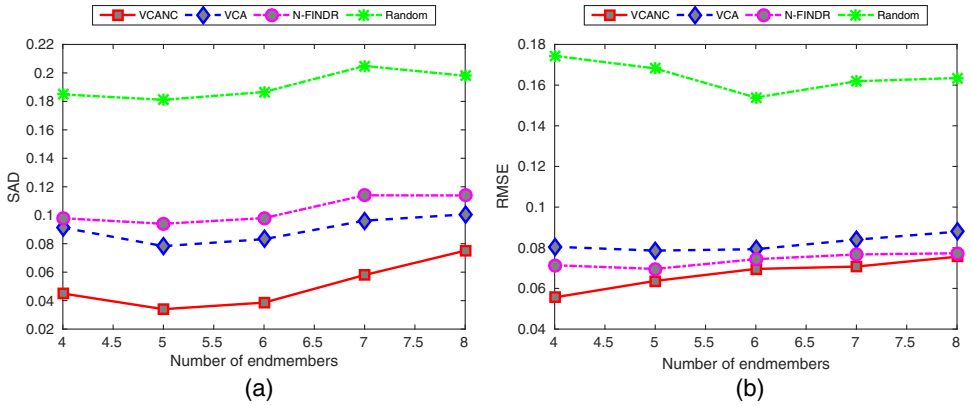

Fig. 3 Comparison of the algorithms with different numbers of endmembers (SD2). (a) SAD and (b) RMSE.

4.1.5 *Experiment 4 (comparison with NMFupk)*

In this experiment, we compare the performance of NMFupk and the NMF-based unmixing method using the VCANC initialization with SD3. The experimental results are demonstrated in Fig. 4. We can see that the performance of NMFupk is improved as the number of the known endmembers increases. The performance of VCANC is nearly the same as that of NMFupk with three known endmembers. It is well known that the known endmembers are not available in many practical situations, so NMFupk is not applicable in real scenes, while VCANC is

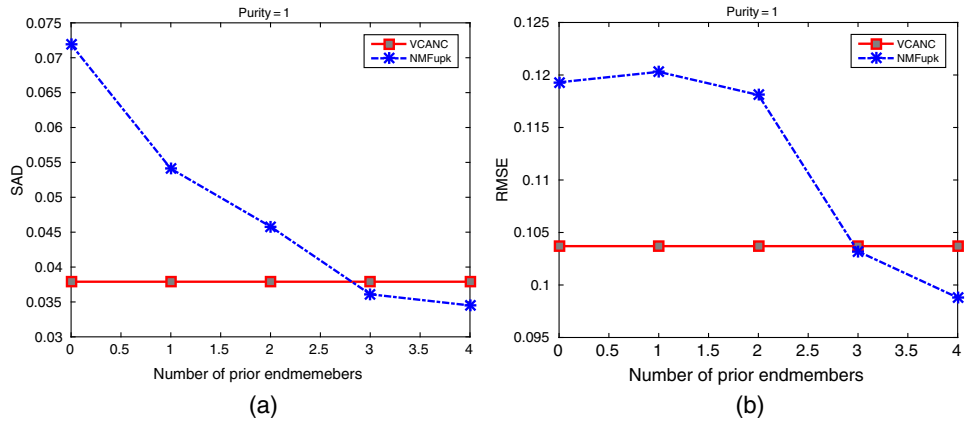

Fig. 4 Comparison of VCANC and NMFupk with different numbers of known endmembers (SD3). (a) SAD and (b) RMSE.

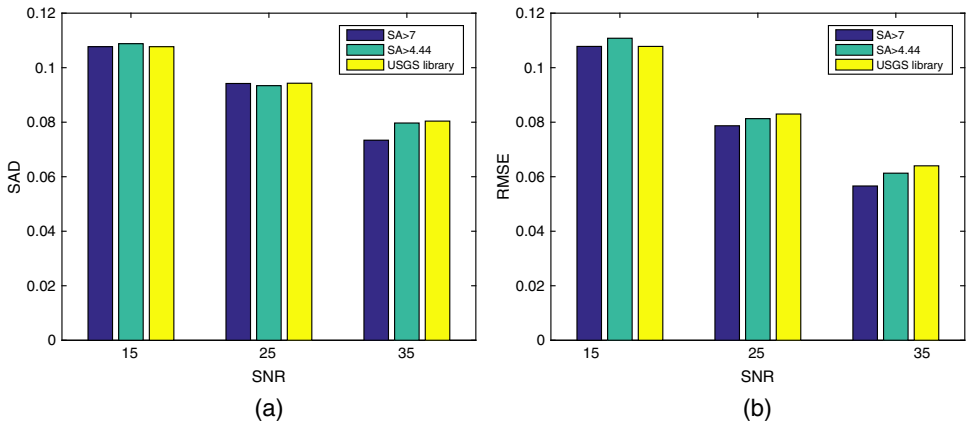

Fig. 5 Influence of different mutual coherence. (a) SAD and (b) RMSE.

able to solve this problem by obtaining initial endmembers, which include the true endmembers identified from the spectral library. It provides a more accurate initial point since it is closer to the global optimization. The performance of NMF-based unmixing can be improved with the VCANC initialization when there are no known endmembers.

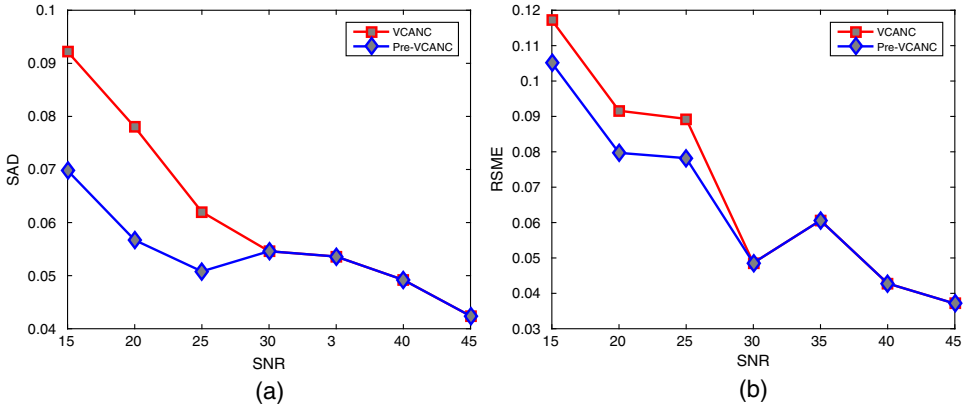

Fig. 6 Spectral variation alleviation. (a) SAD and (b) RMSE.

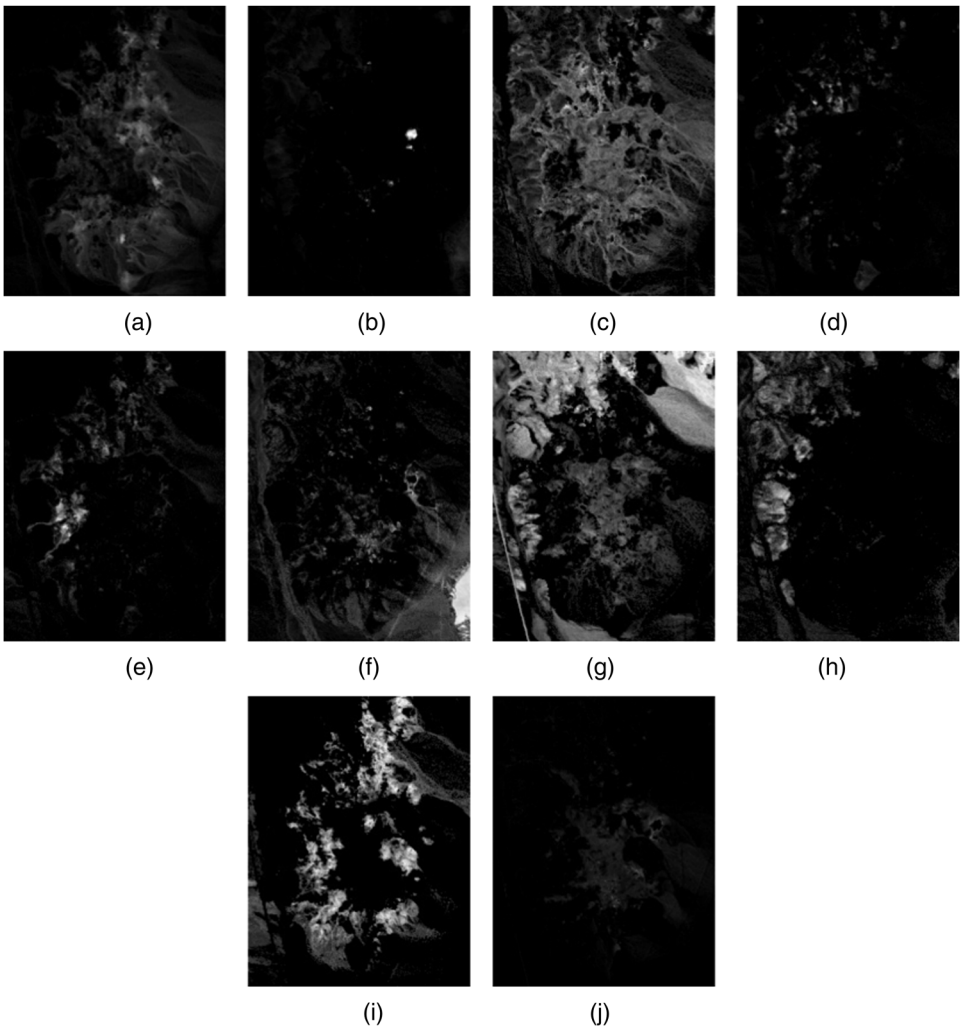

Fig. 7 Unmixing results for the Cuprite data set using VCANC. (a) Alunite. (b) Muscovite. (c) Nortronite. (d) Kaolinite 1. (e) Buddingtonite. (f) Montmorillonite. (g) Desert varnish. (h) Sphene. (i) Kaolinite 2. (j) Chalcedony.

4.1.6 *Experiment 5 (mutual coherence effect on the initialization)*

This experiment aims at evaluating the stability of VCANC when the mutual coherence of the spectral library changes. Three libraries are used in the experiment, among which the initial one is the USGS spectral library whose mutual coherence is very close to 1. The other two libraries are constructed through retaining a fixed number of signatures from the initial library. Spectral signatures in one library are quite different where their spectral angles are larger than 7 deg, as well as the other library whose spectral angle is no smaller than 4.44 deg, indicating that the spectral signatures can be easily confused. In this experiment, $\mathbf{W}_{\mathrm{NC}}$ of SD1 is estimated using these three spectral libraries when SNR is assigned to 15, 25, and 35 dB. Figure 5 shows the plots of the unmixing results. We can see that the unmixing results will be slightly affected by mutual coherence at different noise levels.

4.1.7 *Experiment 6 (spectral variation alleviation)*

Spectral variation which widely exists in hyperspectral data degrades the performance of hyperspectral analysis, such as endmember extraction in this paper. To alleviate the spectral variation, a preprocessing step introduced in Ref. 22 is considered before VCANC, during which the hyperspectral data is decomposed into a low-rank matrix corresponding to intrinsic spectral features and a sparse matrix related to the spectral variation. Then VCANC only works on the low-rank matrix. We compare the performance of the original VCANC with that of the VCANC with preprocessing (Pre-VCANC) using SD1. The experimental results are demonstrated in Fig. 6. We can see that the performance of VCANC is obviously improved by alleviating the spectral variation, which is caused by the heavy noise in the simulated data.

4.2 *Experiments on Real Hyperspectral Data*

We apply the proposed method to unmix a real hyperspectral image captured by AVIRIS in June 1997 over Cuprite, Nevada. This data set has 224 bands, covering the wavelength range of 0.37 to 2.48 μm with a spectral resolution of 10 nm, which is very appropriate for evaluating the

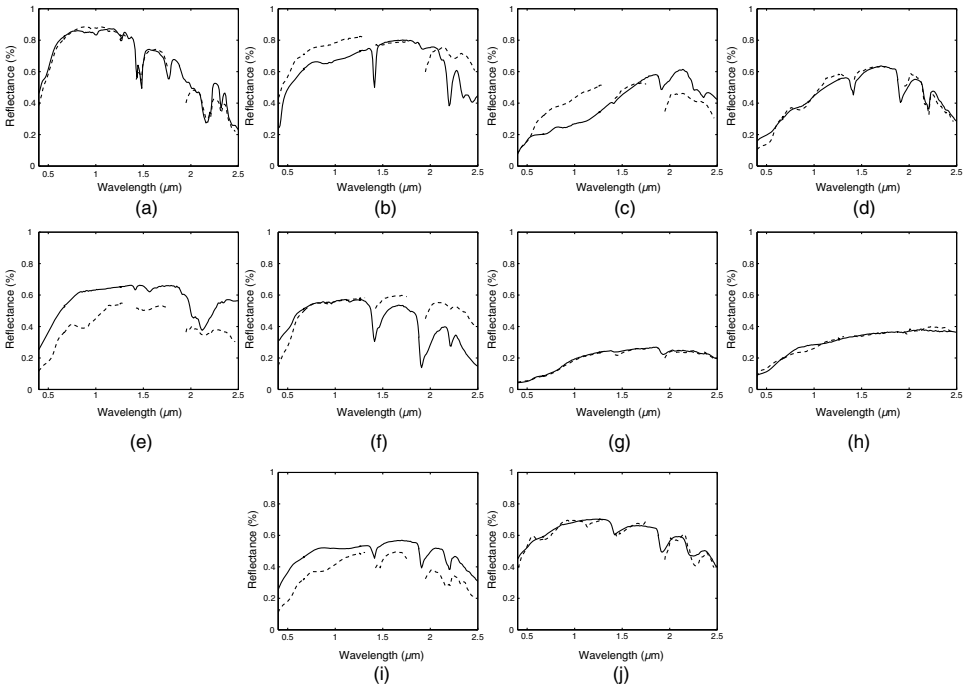

Fig. 8 Results on the AVIRIS Cuprite image: Comparison of the (solid line) USGS library spectra with the (dotted line) signatures extracted by VCANC. (a) Alunite. (b) Muscovite. (c) Nortronite. (d) Kaolinite 1. (e) Buddingtonite. (f) Montmorillonite. (g) Desert varnish. (h) Sphene. (i) Kaolinite 2. (j) Chalcedony.

Table 3 SAD Comparison for the Cuprite data set.

Mineral	VCANC	NMFupk	VCA	N-FINDR
Alunite	**0.0334**	0	0.0976	0.1570
Muscovite	0.1338	**0.1301**	0.1306	0.1358
Nortronite	0.2887	0.2771	0.2815	**0.1660**
Kaolinite 1	**0.0448**	0	0.0989	0.0858
Buddingtonite	**0.0511**	0.1264	0.1096	0.0835
Desert varnish	0.2130	0.2305	0.2317	**0.2110**
Montmorillonite	**0.0428**	0.2004	0.2145	0.0867
Sphene	**0.0606**	0.0608	0.0797	0.0591
Kaolinite 2	**0.1371**	0.1383	0.1390	0.1358
Chalcedony	**0.0311**	0.1274	0.1541	0.1831

Note: The numbers in bold represent the best performance.

performance of unmixing, because the minerals are normally highly mixed. Prior to unmixing, the bands with low SNR and water vapor absorption (including bands 1–2, 104–113, 148–167, and 221–224) are removed, leaving 188 bands. According to the previous analysis,[23] 12 types of minerals are presented in this scene. It is worth mentioning that the variants of the same mineral with slightly different spectra can be considered as the same endmember, hence, r is set to 10. In addition, the threshold th is kept at 0.990.

Figure 7 illustrates the estimated abundances by the proposed method and Fig. 8 shows the comparison between the extracted endmember signatures by the proposed method and their corresponding USGS library spectra. Table 3 shows the quantitative results of different methods in terms of SAD. It is shown that the proposed method demonstrates better performances for a large variety of the minerals compared to the other methods. This is because there are five endmembers (Kaolinite 1, Chalcedony, Alunite, Buddingtonite, and Montmorillonite), which are found by the proposed method during the initialization process. It is expected that accurate initialization gives an accurate initial point and reduces the SAD between the estimated endmember signatures and the USGS library spectra.

5 Conclusion

In this paper, an initialization method for hyperspectral image unmixing has been proposed. The proposed method determines the initial endmembers from both a real-observed hyperspectral image and a spectral library by combining unsupervised VCA and a norm change method. To locate the endmembers from the spectral library, we also propose the use of a nuclear norm change of the abundance matrix. It is interesting to find that for the statistical-based unmixing approaches, the more true endmembers that can be estimated in the initialization stage, the better performance for postspectral unmixing. Our proposed method can find more true endmembers in the initialization stage and enables a better performance for spectral unmixing compared to current popular initialization methods. Experimental results on both simulated and real hyperspectral images demonstrate that the proposed method outperforms other initialization methods in hyperspectral unmixing.

Acknowledgments

This work was supported by China Scholarship Council, the FWO project G037115N: Data fusion for image analysis in remote sensing and the National Natural Science Foundation of China under Grant 61371165.

References

1. N. Keshava and J. F. Mustard, "Spectral unmixing," *IEEE Signal Process. Mag.* **19**(1), 44–57 (2002).
2. J. M. Bioucas-Dias et al., "Hyperspectral unmixing overview: geometrical statistical, and sparse regression-based approaches," *IEEE J. Sel. Top. Appl. Earth Obs. Remote Sens.* **5**(2), 354–379 (2012).
3. M. E. Winter, "N-FINDR: an algorithm for fast autonomous spectral end-member determination in hyperspectral data," *Proc. SPIE* **3753**, 266 (1999).
4. J. M. P. Nascimento and J. M. Bioucas-Dias, "Vertex component analysis: a fast algorithm to unmix hyperspectral data," *IEEE Trans. Geosci. Remote Sens.* **43**(4), 898–910 (2005).
5. J. Li and J. M. Bioucas-Dias, "Minimum volume simplex analysis: a fast algorithm to unmix hyperspectral data," in *IEEE Int. Geoscience and Remote Sensing Symp. (IGARSS'08)*, pp. 250–253 (2008).
6. T. H. Chan et al., "A convex analysis-based minimum-volume enclosing simplex algorithm for hyperspectral unmixing," *IEEE Trans. Signal Process.* **57**(11), 4418–4432 (2009).
7. D. C. Heinz and C. I. Chang, "Fully constrained least squares linear spectral mixture analysis method for material quantification in hyperspectral imagery," *IEEE Trans. Geosci. Remote Sens.* **39**(3), 529–545 (2001).
8. J. Wang and C. I. Chang, "Applications of independent component analysis in endmember extraction and abundance quantification for hyperspectral imagery," *IEEE Trans. Geosci. Remote Sens.* **44**(9), 2601–2616 (2006).
9. W. Xia et al., "Independent component analysis for blind unmixing of hyperspectral imagery with additional constraints," *IEEE Trans. Geosci. Remote Sens.* **49**(6), 2165–2179 (2011).
10. V. P. Pauca, J. Piper, and R. Plemmons, "Nonnegative matrix factorization for spectral data analysis," *Linear Algebra Appl.* **416**(1), 29–47 (2006).
11. L. D. Miao and H. R. Qi, "Endmember extraction from highly mixed data using minimum volume constrained nonnegative matrix factorization," *IEEE Trans. Geosci. Remote Sens.* **45**(3), 765–777 (2007).
12. S. Jia and Y. T. Qian, "Constrained nonnegative matrix factorization for hyperspectral unmixing," *IEEE Trans. Geosci. Remote Sens.* **47**(1), 161–173 (2009).
13. A. Plaza and C. I. Chang, "Impact of initialization on design of endmember extraction algorithms," *IEEE Trans. Geosci. Remote Sens.* **44**(11), 3397–3407 (2006).
14. X. Q. Lu et al., "Manifold regularized sparse NMF for hyperspectral unmixing," *IEEE Trans. Geosci. Remote Sens.* **51**(5), 2815–2826 (2013).
15. X. T. Tao et al., "A new scheme for decomposition of mixed pixels based on nonnegative matrix factorization," in *IEEE Int. Geoscience and Remote Sensing Symp.*, pp. 23–28 (2007).
16. W. Tang, Z. W. Shi, and Z. Y. An, "Non-negative matrix factorization for hyperspectral unmixing using prior knowledge of spectral signatures," *Opt. Eng.* **51**(8), 087001 (2012).
17. M. D. Iordache, J. M. Bioucas-Dias, and A. Plaza, "Sparse unmixing of hyperspectral data," *IEEE Trans. Geosci. Remote Sens.* **49**(6), 2014–2039 (2011).
18. D. D. Lee and H. S. Seung, "Algorithms for non-negative matrix factorization," in *Proc. of Advances in Neural Information Processing Systems*, pp. 556–562 (2001).
19. E. J. Candes et al., "Robust principal component analysis?," *J. ACM* **58**(3), 11 (2011).
20. M. D. Iordache, J. M. Bioucas-Dias, and A. Plaza, "Collaborative sparse regression for hyperspectral unmixing," *IEEE Trans. Geosci. Remote Sens.* **52**(1), 341–354 (2014).
21. Y. T. Qian et al., "Hyperspectral unmixing via $l_{1/2}$ sparsity-constrained nonnegative matrix factorization," *IEEE Trans. Geosci. Remote Sens.* **49**(11), 4282–4297 (2011).
22. S. Mei et al., "Spectral variation alleviation by low-rank matrix approximation for hyperspectral image analysis," *IEEE Geosci. Remote Sens. Lett.* **13**(6), 796–800 (2016).
23. X. T. Tao, B. Wang, and L. M. Zhang, "Orthogonal bases approach for the decomposition of mixed pixels in hyperspectral imagery," *IEEE Geosci. Remote Sens. Lett.* **6**(2), 219–223 (2009).

Rui Wang received her BS and MS degrees in information engineering from the Southwest Jiaotong University, Chengdu, China, in 2002 and 2008, respectively. Currently, she is pursing her PhD at the School of Information Science and Technology, Southwest Jiaotong University, Chengdu, China. Her research interests include hyperspectral image analysis and processing.

Hengchao Li received his PhD in signal and information processing from the Institute of Electronics, Chinese Academy of Sciences, Beijing, China, in 2008. Currently, he is a professor with Sichuan Provincial Key Laboratory of Information Coding and Transmission from 2012 and also is a PhD supervisor from 2013. His research interests include remote sensing image analysis, processing and applications.

Wenzhi Liao received his BS degree in mathematics from Hainan Normal University, Haikou, China, in 2006, and his PhD in engineering from South China University of Technology, Guangzhou, China, in 2012, and his PhD in computer science engineering from Ghent University, Ghent, Belgium, in 2012. Since 2012, he has been a postdoctoral researcher with Ghent University. His research interests include mathematical morphology, multitask feature learning and multisensor data fusion.

Xin Huang received his PhD in photogrammetry and remote sensing from Wuhan University, Wuhan, China, in 2009, working with the State Key Laboratory of Information Engineering in Surveying, Mapping and Remote Sensing (LIESMARS). He is currently a full professor with LIESMARS. He has published more than 50 peer-reviewed articles in international journals. His research interests include hyperspectral data analysis, high-resolution image processing, pattern recognition, and remote sensing applications.